In silico prediction of some pharmacokinetic, safety, biological activity and molecular docking studies of 1-piperazine indole hybrid with nicotinic amide and nicotinic acid and their analogues

Melese Legesse Mitku[1] (iD), Abera Dessie Dagnaw[1] (iD),
Derso Teju Geremew[2], Yeniewa Kerie Anagaw[1] (iD),
Minichil Chanie Worku[1], Liknaw Workie Limenh[2] (iD),
Yabibal Berie Tadesse[1] and Asrat Elias Ergena[1]

Abstract

Background: In silico predictions are now being utilized in drug discovery and design to assess the physicochemical, pharmacokinetics, and safety properties of compounds at the beginning of the drug discovery process. This early evaluation of the physicochemical, pharmacokinetics, and safety properties of compounds helps the researchers to invest their time and resources only in the best prospective lead compounds by eliminating compounds with a low chance of success.

Objective: The purpose of this study was to explore a promising lead compound designed from 1-piperazine indole hybrid with nicotinic amide and nicotinic acid analogs targeted on *Trypanosoma brucei* phosphofructokinase for Trypanosomiasis activity by using in silico predictions strategy.

Results: The physicochemical, safety, pharmacokinetic, and biological activity properties of those molecules were predicted by using ADMETlab 2.0, ACD labs Chem Sketch software version 14.0, Molinspiration software, and MolPredictX online tool. Our results indicate that several promising candidates exhibit favorable characteristics. Based on Molinspiration software both nicotinic acid and nicotinic amide derivatives showed higher kinase inhibitor activity and all nicotinic acid derivatives revealed enzyme inhibitors and GPCR ligand activity. According to the MolPredictX online tool, the most biologically active derivatives were NA-4, NA-11, and NAD-11.

Conclusion: Overall, our findings offer valuable insights into the potential efficacy and safety of these compounds. It appears that almost all of the compounds have successfully passed the pharmacokinetic evaluations and integration of nicotinic acid into indole appears to be more beneficial than nicotinic amide regarding certain biological activities.

Keywords
Biological activity, in silico, indole, molecular docking, pharmacokinetics, safety

Introduction

Heterocycles are a relatively prevalent component of many active pharmaceutical compounds in the field of medicinal chemistry.[1,2] The indole moiety is one of the most widespread heterocycles found in natural products, and it also has a very critical role in the design of new biologically active molecules.[3–5] Indoles and compounds containing indole scaffolds displayed a wide range of biological activities.[6,7] They

[1]Department of Pharmaceutical Chemistry, School of Pharmacy, College of Medicine and Health Sciences, University of Gondar, Gondar, Ethiopia
[2]Department of Pharmaceutics, School of Pharmacy, College of Medicine and Health Sciences, University of Gondar, Gondar, Ethiopia

Corresponding author:
Melese Legesse Mitku, Department of Pharmaceutical Chemistry, School of Pharmacy, College of Medicine and Health Sciences, University of Gondar, P.O. Box 196, Gondar 6200, Ethiopia.
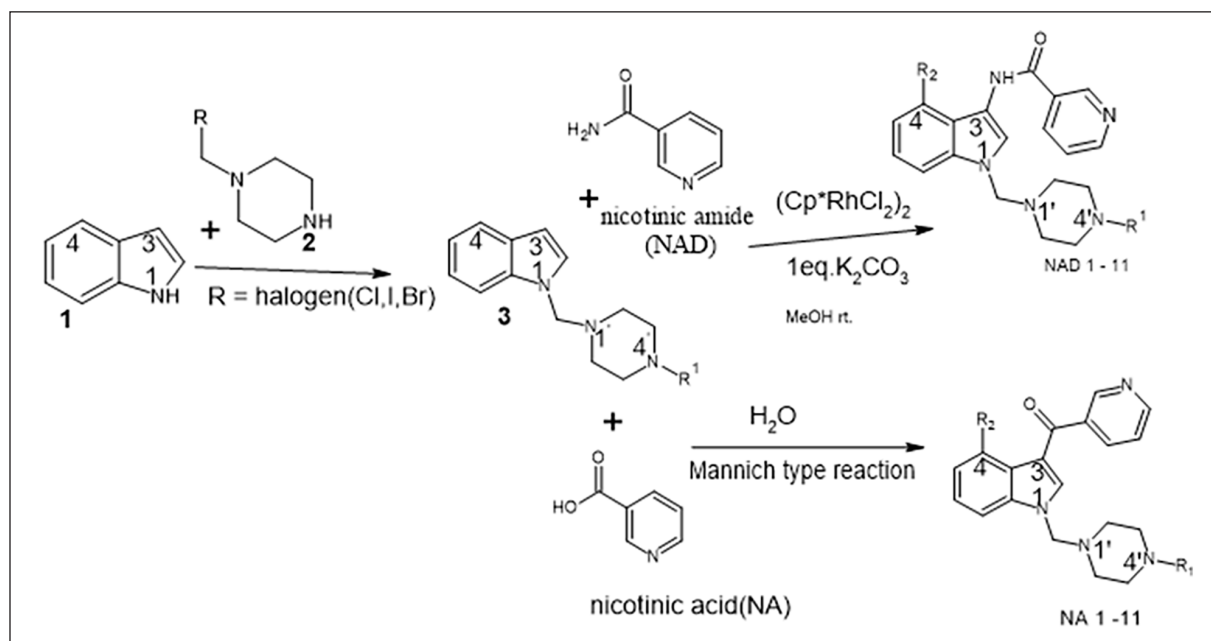Email: melese.5legesse@gmail.com

Figure 1. Proposed synthesis of indoles derived from nicotinic amide and nicotinic acid agents.

showed important biological activities, including anticancer,[8] antioxidant, anti-inflammatory, antifungal, anticholinesterase, and antibacterial properties.[9] Many indole-based synthetic medications have recently been discovered, and they display various biological activities.[10] Among the indole class of compounds, 1,3-, and 4-trisubstituted indoles appear to be the most promising lead compounds for drug development.[11]

Numerous reviews of the literature suggest that nicotinic acid and its derivatives exhibit a wide range of biological properties, such as antioxidant,[12] antitubercular, anticancer,[13] analgesic, and anti-inflammatory[14] effects. Additionally, the nicotinic acid moiety of nicotinic acid has been incorporated into several compounds with antimicrobial activity against a variety of pathogens, including resistant strains.[15]

Furthermore, it has been shown that compounds containing nicotinic amide derivatives have important biological effects. These effects include the treatment of ischemic and traumatic brain injury, as well as antioxidant,[16] anticancer, antifungal, antimicrobial, antibacterial, and antibiofilm properties of some nicotinamide derivatives.[17] Thus, the hybridization of nicotinic acid and nicotinic amide with indole as a single entity produces a more active biological product.

Figure 1 illustrates the proposed mechanism for generating compounds (NAD 1-11 and ND 1-11) that include indole from nicotinic amide and nicotinic acid agents. Indoles have extremely reactive positions at positions 1, 3, and 4, with position 3 (C3) being the most reactive,[18–20] and the selection of these positions 1 (R_1), 3, and 4 (R_2) are based on previously published articles.[21,22] In the synthesis of N-substituted indoles with bioactivity compounds, the indoles normally serve as nucleophilic coupling partners to react with diverse

electrophiles, such as activated olefins, ketones, imines, alkyl halide, and alkynes.[23] Thus, we select N-methyl halide piperazine in this reaction strategy. In this first step is N-methyl halide piperazine (2) undergoing the electrophilic aromatic substitution reaction with indole moiety (1) on position 1, this gives 1-(piperazin-1-ylmethyl)-1H-indole (3), typically in good yields.[24] The 3-portion of compound 3 undergoes an electrophilic aromatic substitution process to react with molecules that have carbonyl functional group[15] like nicotinic acid (NA), and this gives indole-based NA derivatives and also an effective strategy for oxidative cross-coupling of indoles with various ketones is based on a via, a well-known Mannich-type reaction forming indole-based NA derivatives.[25] The 3-potion of compound 3 also undergoes electrophilic amidation using the electrophilic nitrogen source and provides 3-indole-based NAD derivatives.[26,27] Additionally, position 4 of indole and position 4' of piperazine both undergo an electrophilic substitution reaction with alkyl halides to provide indole-based derivatives NAD1-6 and NA1-6, as well as NAD7-11 and NA7-11, respectively.

The primary cause of potential lead candidate compounds' failure was the late-stage discovery of their pharmacokinetics and safety properties.[28] A recent study identified inadequate pharmacokinetics, preclinical toxicity, and a lack of efficacy as the main causes of lead candidate compound failures.[29] In silico predictions are now being utilized in drug discovery and design to assess the physicochemical, pharmacokinetics, and safety properties of compounds at the beginning of the drug discovery process. The researcher will be able to pick the best prospective lead candidate compounds for development and eliminate those with a low chance of success, thanks to this early evaluation of pharmacokinetics

and safety profiles.[30] Thus, in silico predictions reduce late-stage failures of promising lead candidate compounds by focusing on their desired pharmacokinetics and safety properties.[31–33] This study aimed to explore a promising lead compound targeted on TbPFK for Trypanosomiasis activity generated from 1-piperazine indole hybrid with nicotinic amide and nicotinic acid and their analogs by in silico predictions of the selective physicochemical and pharmacokinetics, safety, and molecular docking properties. In this study, we have first in silico predicted physicochemical properties such as molecular weight (MW), aqueous solubility (LogS), lipophilicity (LogP), and n-octanol/water distribution (LogD), and molecular properties such as the number of hydrogen bond acceptors (nHA), number of hydrogen bond donors (nHD), topological polar surface area (TPSA), number of rotatory bonds (nRot), number of the ring (nRing), and chiral center (Stereo Centers) of compounds NAD 1-11 and ND 1-11 properties. Then, we have predicted the pharmacokinetic properties (absorption, distribution, metabolism, and excretion), and toxicity (such as hERG for cardiotoxicity, DILI for hepatotoxicity, Ames for mutagenicity, eye irritation, and carcinogenicity) of compounds. Lastly, we have in silico predicted bioactivity scores of the most common drug targets (GPCR ligands, ion channel kinase inhibitors, nuclear inhibitors, protease inhibitors, and enzyme inhibitors), biological activities (such as Trypanosoma and Leishmania), and molecular docking studies of compounds (NAD 1-11 and NA 1-11).

Here, we first selected nicotinic amide and nicotinic acid as lead compounds, then we synthesized drug-like substituted indole compounds in an ideal way. Based on these data, we made in silico predictions regarding the physicochemical, pharmacokinetic, toxicity, key targets, and biological activity of these compounds. Selected physicochemical (LogS, LogP, and LogD), molecular (Mw, TPSA), pharmacokinetic (Caco-2, BBB, VD, CYP, and Cl), and toxicity (mutagenicity, cardiotoxicity, irritant action, and carcinogenicity), and biological activity properties were predicted using software such as ACD labs chemsketch version 12.0, ADMETlab 2.0, Molinspiration, and MolPredictX online program for prediction of activity spectrum of substances.[34]

Materials and method

Lead compounds

A "lead compound" is a chemically modified compound that is used to synthesize other compounds to improve target specificity, bioavailability, and pharmacokinetics, as well as achieve optimal therapeutic activity. These compounds are then tested for their therapeutic activity through preclinical and clinical studies.[35,36] As it aids in optimizing pharmacokinetics and pharmaceutical characteristics, drug-likeness is a crucial factor to take into account when choosing compounds in the early stages of the drug-discovery process. These consist of distribution patterns, bioavailability, solubility, and

chemical stability.[37] Thus, we selected nicotinic amide and nicotinic acid as lead molecules to create some drug-like substituted indole molecules.

Drug-like molecules

Nicotinic amide and nicotinic acids were used to synthesize certain drug-like substituted indoles. Using ACD/Chemsketch software, the structures of these drug-like substituted indoles were created. ACD research facilities ACD labs ChemSketch v 14.0 is a chemical drawing software package designed to assist chemists in designing professional reports and presentations as well as quickly and easily drawing chemical structures of organic molecules, IUPAC names, 3D structures, molecular properties, physicochemical properties, reactions, and schematic diagrams, which are available at https://chemsketch. software.informer.com/14.0.[38] All these chemical structures were saved and exported to ADMETlab 2.0 online software, Molinspiration, and MolPredictX.

Prediction of physicochemical, pharmacokinetic, and toxicity profile of compounds NAD 1-11 and ND 1-11

In silico prediction of the physicochemical, pharmacokinetic properties, and toxicity profiles of indole[1] and its derivative's absorption, distribution, metabolism, excretion, and toxicity were estimated using ADMETlab 2.0 (https://admet-mesh.scbdd.com/)[39] online software.

Prediction of the primary pharmacological targets

The prediction of bioactivity score for the most important drug targets such as GPCR ligands, kinase inhibitors, ion channel modulators, enzymes, and nuclear receptors was made using Molinspiration software. Molinspiration is a free online service for the prediction of bioactivity scores for the most important drug targets and calculation of important molecular properties such as Molinspiration Log P, polar surface area, number of hydrogen bond donors (HBD), and acceptors (HBA) and others.[40]

The prediction of SAR of compounds

Structural-activity relationships of the compounds were accomplished using online program software. Structures of the compounds were drawn through. Chem Sketch software was submitted to the MolPredictX online program and predicted the possible biological activities.[34]

Molecular docking

Molecular docking techniques are among the most successful tactics for predicting medication interactions with macromolecules. The docking process entails looking for binding

sites over the macromolecule's whole surface.[41] The molecular docking study of the compounds was carried out using the Glide docking module of the Schrödinger suite 2023 version 1 (Schrödinger Inc., New York, NY, USA). Biologically active compounds molecular docking studies were done on TbPFK. The crystal structure of *T. brucei PFK is* bound with a natural product CTCB-405(JJ2) (PDB: 6QU4) and used as a template for the docking.

Protein preparation

In this study, the structure of the Trypanosoma receptor protein (PDB: 6QU4) was obtained from the Protein Data Bank (http://www.rcsb.org).[42] Then, the protein was prepared using the protein preparation wizard by using the Maestro Schrödinger suite 2023 version 1. The protein structure from PDB is imported to the protein preparation wizard in Maestro. From the PDB structure, along with other various missing details regarding specific connections, the bond orders and formal changes are absent. The steps of protein preparation are as follows.

The initial stage of protein preparation is called preprocessing, and it is important for subsequent actions related to structure preparation, including the generation of heteroamorous states, the assignment of H bonds, and the degree of minimization. The preprocessing stage in the protein preparation wizard has numerous options.

Such as the protein was prepared by filling missing residues in the area around the binding site of protein (6QU4); by assigning bond orders, adding any missing hydrogen atoms, creating disulfide bonds, and removing water molecules longer than 5 Å.

The second stage of protein preparation is optimization. This is an interactive optimization that allows different clusters of hydrogen-bonded species to be efficiently optimized, as well as an automatic optimization that operates on all H-bonds (with or without the presence of water molecules). Reducing the structure has been done so deliberately and moderately in order to refine it. In particular, the atom's RMSD value was kept to a minimum in Angstrom. Also, the optimal potentials for Liquid Simulations (OPLS3e) force fields were used to compute the partial atomic charges in an efficient manner.[43]

Ligand preparation

The ligand compounds were prepared using the LigPrep wizard in Maestro Schrödinger suites. Ligand structure preparation, or LigPrep, is a robust set of tools that was created specifically to create high-quality, all-atom 3D structures for a large number of molecules that resemble drugs. 2D or 3D structures of active compounds for docking study were constructed using the SKETCH option in Maestro. The structures can be created in 2D or 3D dimensions using the Structures Data File (SDF) or Maestro formats. The ionization states and tautomer were produced. Furthermore, energy minimization of the ligands was carried out, and minimizing macromolecular structures was used by the OPLS3e force field.

Preparation of grid generation and docking poses

The grid box can be generally generated by utilizing the receptor grid generation. Docking of ligand cannot be performed before the grid generation step. To prepare and select the binding site for the docking, Glide was applied to generate a grid by selecting atoms of the bound ligand, CTCB-405(JJ2) in a 20 Å. Protein structures with the proper bond arrangement and formal charges had to be generated to generate receptor grids. Four tabs are available in the receptor grid creation, which is used to create a grid. They are names as Receptor, Site, constraints, and Rotatable Groups.

A receptor is a component of a system that is located in the workspace. Either an entry or a molecule in the workspace can be recognized as the ligand. The default values for the scaling factor and partial charge cut-off are 0.30 and 0.25, respectively. The default values of the charge scale factor and the Van der Waals radius scale factor are 1.0. Based on a pH of 7.4 ± 1.0, the protonation states of ligands were computed.

Next, choose site, which indicates where the scoring grids are located and how to get ready from the workspace's structure. Site is defined as the collection of site points on a certain grid that is in contact with extremely tiny gaps in the solvent-exposed regions. The definition of the enclosing box, also known as the outer box, is the grid's evaluation inside the designated space—atoms of ligands are inside the box.

The receptor grid will be generated once you pick the site and press constraints. It was done with glide constraints. H-bond or metal, positional, and hydrophobic are the three subtabs that make up the constraints. To keep the majority of the receptor hidden and only reveal the residues that are close to the ligand, constraint settings may be helpful.

Finally, we choose rotatable groups. Glide's rotatable groups are utilized to adopt various hydroxyl group orientations with various ligands. When creating the receptor grid, it is important to handle the rotatable hydroxyl groups with flexibility.
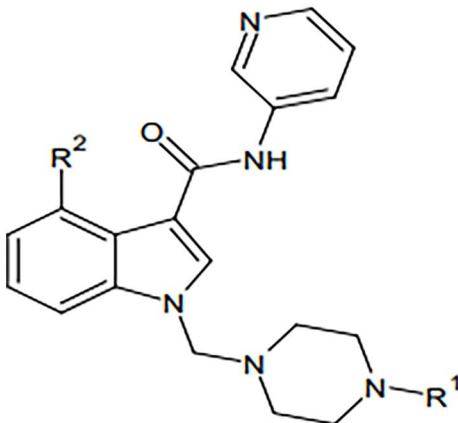
One of the Schrödinger suites, GLIDE (Grid-based Ligand Docking with Energetic), is employed in the docking analysis. GLIDE looks for areas of the protein where the ligands and protein interact well. They were then docked by Glide extra precision (XP).[44,45] GLIDE XP is designed for use only on good ligand poses. XP mode has docked only the top-scoring ligands. The top dock score poses of the compounds were further analyzed and visually inspected using PyMOL version 2.5 to examine their detailed binding interaction.

Results
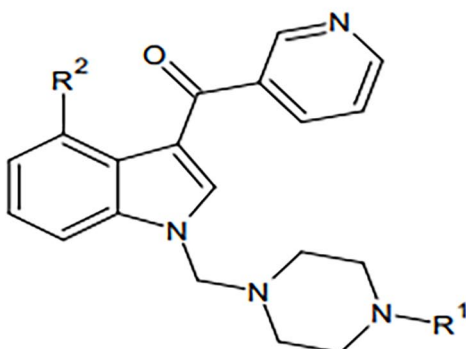
Physicochemical, pharmacokinetic, and toxicity profile of compounds NAD 1-11 and ND 1-11

The results of physicochemical, molecular properties, pharmacokinetic, and toxicity studies of indole hybrid with nicotinic amide and nicotinic acid and their analogs were predicted by using ADMETlab 2.0 online software tool (https://admetmesh.scbdd.com/) and reported in Tables 1 and 2, respectively.

Table 1. In silico prediction results of physicochemical and molecular properties of compounds NAD 1-11 and ND 1-11 (ADMETLab2.0).

NAD1-11 NA1-11

Code	R₁	R₂	Mw	LogS	LogD	LogP	nHA	nHD	TPSA	nRot	nRing	Stereo centers	LRO5	QED
NAD1	H	H	335.17	−2.503	2.079	1.432	6	2	62.19	5	4	0	Accepted	0.767
NAD2	CH₃	H	349.19	−2.766	2.327	2.001	6	1	53.4	5	4	0	Accepted	0.786
NAD3	CH₂CH₃	H	363.21	−3.006	2.63	2.557	6	1	53.4	6	4	0	Accepted	0.757
NAD4	COCH₃	H	377.19	−2.86	2.033	1.663	7	1	70.47	6	4	0	Accepted	0.758
NAD5	CONH₂	H	378.18	−2.64	1.883	1.306	8	3	96.49	6	4	0	Accepted	0.725
NAD6	CONHCH₃	H	392.2	−3.277	2.169	1.552	8	2	82.5	7	4	0	Accepted	0.713
NAD7	H	Cl	369.14	−3.141	2.655	2.052	6	2	62.19	5	4	0	Accepted	0.742
NAD8	H	F	353.17	−2.35	2.236	1.563	6	2	62.19	5	4	0	Accepted	0.756
NAD9	H	CH₃	349.19	−2.386	2.378	1.798	6	2	62.19	5	4	0	Accepted	0.76
NAD10	H	CF₃	403.16	−2.972	3.013	2.4	6	2	62.19	6	4	0	Accepted	0.703
NAD11	H	NO₃	380.16	−3.304	1.969	1.383	9	2	105.33	6	4	0	Accepted	0.518
NA1	H	H	320.16	−1.894	1.758	1.213	5	1	50.16	4	4	0	Accepted	0.748
NA2	CH₃	H	334.18	−2.074	2.009	1.78	5	0	41.37	4	4	0	Accepted	0.688
NA3	CH₂CH₃	H	348.2	−2.365	2.352	2.337	5	0	41.37	5	4	0	Accepted	0.665
NA4	COCH₃	H	362.17	−1.99	1.67	1.41	6	0	58.44	5	4	0	Accepted	0.669
NA5	CONH₂	H	363.17	−2.598	1.82	1.381	7	2	84.46	5	4	0	Accepted	0.718
NA6	CONHCH₃	H	377.19	−2.598	1.82	1.381	7	1	70.47	6	4	0	Accepted	0.708
NA7	H	Cl	354.12	−2.774	2.399	1.849	5	1	50.16	4	4	0	Accepted	0.732
NA8	H	F	338.15	−1.9	1.96	1.424	5	1	50.16	4	4	0	Accepted	0.742
NA9	H	CH₃	334.18	−2.002	2.123	1.679	5	1	50.16	4	4	0	Accepted	0.745
NA10	H	CF₃	388.15	−2.524	2.824	2.175	5	1	50.16	5	4	0	Accepted	0.698
NA11	H	NO₃	365.15	−2.891	1.669	1.238	8	1	93.3	5	4	0	Accepted	0.422

Targets and biological activity spectrum prediction of compounds (NAD 1-11 and NA 1-11)

The result of the bioactivity score for the most important drug targets of compounds (NAD 1-11 and NA 1-11) was predicted by using Molinspiration online tools and reported in Table 3. As Table 3 shows nicotinic acid derivatives NA1-11 had the highest kinase inhibitor score (0.21–0.40), followed by nicotinic amide derivatives NAD1-11 that had a higher kinase inhibitor score (0.11–0.28). Compounds NA1-11 had also moderate enzyme inhibitors (0.07–0.25) and GPCR ligands (0.01–0.25) activity. Compounds NAD1 (0.03) and NAD6-10 (0.01–0.09) had weak GPCR ligand and enzyme inhibitors NAD1, and NAD5-10 (0.01–0.09) activity. All nicotinic acid and nicotinic amide derivatives

Table 2. Pharmacokinetic and toxicity profile of compounds NAD 1-11 and NA 1-11 (ADMETLab2.0).

Comp	Caco-2	MDCK	F20%	BBB	PPB (%)	VD	CYP3A4 inhi	CYP3A4 subst	CL	T1/2	hERG	DILI	Ames	Carcinogenicity	Eye irritation
NAD1	−5.629	5.41E-06	0.909	0.971	68.96	2.328	0.182	0.405	7.561	0.14	0.503	0.965	0.347	0.049	0.012
NAD2	−5.04	9.93E-06	0.022	0.991	80.49	2.082	0.165	0.57	10.11	0.084	0.717	0.957	0.327	0.07	0.011
NAD3	−5.076	1.34E-05	0.055	0.988	81.02	1.939	0.135	0.516	11.346	0.064	0.855	0.946	0.478	0.066	0.011
NAD4	−5.304	1.38E-05	0.044	0.872	81.52	1.888	0.181	0.518	2.726	0.186	0.515	0.945	0.11	0.52	0.013
NAD5	−5.439	5.99E-06	0.09	0.942	78.07	1.952	0.134	0.251	4.293	0.141	0.689	0.96	0.181	0.233	0.009
NAD6	−5.509	6.68E-06	0.914	0.974	84.66	1.82	0.371	0.239	4.666	0.201	0.422	0.956	0.154	0.125	0.009
NAD7	−5.628	9.04E-06	0.553	0.944	78.18	2.631	0.464	0.43	7.682	0.148	0.544	0.958	0.298	0.047	0.011
NAD8	−5.631	7.80E-06	0.01	0.967	73.19	2.546	0.294	0.333	7.016	0.145	0.417	0.952	0.599	0.049	0.011
NAD9	−5.639	3.93E-06	0.36	0.967	77.28	2.45	0.277	0.486	7.906	0.189	0.344	0.951	0.523	0.049	0.012
NAD10	−5.63	6.27E-06	0.031	0.833	80.29	3.323	0.382	0.353	6.659	0.095	0.633	0.958	0.529	0.03	0.01
NAD11	−5.618	9.68E-06	0.004	0.695	59.49	2.478	0.204	0.245	6.158	0.221	0.61	0.961	0.984	0.094	0.012
NA1	−5.248	1.52E-05	0.262	0.981	73.54	2.246	0.362	0.405	7.164	0.115	0.56	0.965	0.793	0.062	0.012
NA2	−4.663	1.68E-05	0.011	0.993	79.10	2.177	0.375	0.588	9.272	0.068	0.73	0.953	0.547	0.1	0.011
NA3	−4.777	2.11E-05	0.017	0.992	81.21	2.185	0.281	0.535	10.243	0.051	0.855	0.94	0.637	0.095	0.011
NA4	−4.939	2.48E-05	0.025	0.896	82.79	1.891	0.308	0.541	2.101	0.14	0.531	0.952	0.45	0.75	0.014
NA5	−5.029	1.37E-05	0.012	0.944	75.28	1.96	0.237	0.346	3.47	0.111	0.692	0.966	0.593	0.438	0.01
NA6	−5.156	1.61E-05	0.826	0.973	86.20	1.908	0.58	0.248	3.961	0.169	0.423	0.966	0.524	0.295	0.009
NA7	−5.296	1.71E-05	0.032	0.972	78.04	2.342	0.638	0.515	6.922	0.111	0.658	0.957	0.673	0.059	0.011
NA8	−5.289	1.77E-05	0.007	0.98	73.91	2.475	0.484	0.359	6.357	0.115	0.529	0.947	0.708	0.065	0.011
NA9	−5.34	1.30E-05	0.056	0.982	76.79	2.388	0.484	0.506	7.457	0.15	0.446	0.949	0.828	0.062	0.012
NA10	−5.402	1.12E-05	0.027	0.934	81.22	3.081	0.518	0.377	6.16	0.071	0.736	0.954	0.465	0.035	0.01
NA11	−5.194	4.12E-05	0.004	0.833	61.08	2.509	0.366	0.361	4.396	0.151	0.687	0.96	0.983	0.146	0.012

Log P: partition coefficient; Log S: aqueous solubility, insoluble $<-10<$ poorly $<-6<$ moderately $<-4<$ soluble $<-2<$ very $<0<$ highly; Log D: n-octanol/water distribution coefficients at pH=7.4, 1- 3 considered proper; QED: a measure of drug-likeness based on the concept of desirability: >0.67: excellent (green); ≤0.67: poor (red); F20%: human oral bioavailability 20%; 0–0.3: excellent; 0.3–0.7: medium; 0.7–1.0(++): poor; Caco-2: human colon adenocarcinoma cell lines, >−5.15, proper; BBB: blood–brain barrier, 0–0.3: excellent; 0.3–0.7: medium; 0.7–1.0(++): poor; VD: volume distribution; CYP: cytochrome P450, category 0: nonsubstrate/noninhibitor, category 1: substrate/inhibitor, the probability of being substrate/inhibitor, within the range of 0 to 1; CL: clearance of a drug, 0–0.3: excellent, 0.3–0.7: medium, 0.7–1.0(++): poor; hERG: human ether-a-go-go related gene, 0–0.3: excellent, 0.3–0.7: medium, 0.7–1.0(++): poor; AMES: a test for mutagenicity, 0–0.3: excellent, 0.3–0.7: medium, 0.7–1.0(++): poor; Carcinogencity: 0–0.3: excellent (green); 0.3–0.7: medium (yellow); 0.7–1.0(++): poor (red); DILI: drug-induced liver injury, 0–0.3: excellent, 0.3–0.7: medium, 0.7–1.0(++): poor; EI: eye irritation, 0–0.3: excellent, 0.3–0.7: medium, 0.7–1.0(++): poor.

Table 3. Bioactivity score of the most common drug targets prediction of compounds (NAD 1-11 and NA 1-11) using Molinspiration software.

Compounds	GPCR ligands	Ion channel	Kinase inhibitors	Nuclear inhibitors	Protease inhibitors	Enzyme inhibitors
NAD1	0.03	−0.23	0.22	−0.65	−0.27	0.01
NAD2	0.00	−0.24	0.22	−0.62	−0.31	−0.00
NAD3	−0.01	−0.28	0.14	−0.59	−0.34	−0.03
NAD4	−0.03	−0.34	0.11	−0.66	−0.26	−0.06
NAD5	−0.03	−0.20	0.28	−0.60	−0.17	0.09
NAD6	0.05	−0.18	0.21	−0.66	−0.19	0.04
NAD7	0.01	−0.10	0.20	−0.67	−0.31	0.03
NAD8	0.09	−0.26	0.28	−0.60	−0.29	−0.01
NAD9	0.03	−0.28	0.18	−0.69	−0.36	0.01
NAD10	0.07	−0.18	0.19	−0.45	−0.36	0.02
NAD11	−0.12	−0.29	0.11	−0.67	−0.34	−0.06
NA1	0.19	−0.19	0.34	−0.34	−0.33	0.18
NA2	0.16	−0.20	0.33	−0.32	−0.37	0.16
NA3	0.14	−0.24	0.25	−0.29	−0.39	0.12
NA4	0.09	−0.30	0.21	−0.37	−0.31	0.11
NA5	0.18	−0.16	0.39	−0.32	−0.22	0.25
NA6	0.19	−0.15	0.31	−0.39	−0.23	0.19
NA7	0.16	−0.06	0.31	−0.37	−0.36	0.19
NA8	0.25	−0.22	0.40	−0.31	−0.34	0.15
NA9	0.18	−0.24	0.30	−0.40	−0.41	0.17
NA10	0.21	−0.14	0.30	−0.18	−0.38	0.17
NA11	0.01	−0.27	0.21	−0.41	−0.40	0.07

had no activity on ion channels (−0.06 to −0.29), nuclear inhibitors (−0.18 to −0.69), and protease inhibitors (−0.17 to −0.41).

The results of biological activity spectra were predicted using the MolPredictX computer program[34] as shown in Table 4. As illustrated in Table 4, the most biologically active compounds were nicotinic acid derivative NA-**4** (Tcruzi_amastigota; Pa = 1 and Tcruzi_trypomastigota; Pa = 1), NA-11 (Dengue larvicida; Pa = 1 and Tcruzi_amastigota; Pa = 1), and nicotinic amide derivative NAD-11 (Promastigote Ldonovani; Pa = 1 and Dengue larvicida; Pa = 1). Compounds which have biologically active nicotinic acid derivatives from highest to moderate were NA-10 (Tcruzi_amastigota; Pa = 1 and C_albicans; Pa = 0.6), NAD-2 (Tcruzi_amastigota; Pa = 1 and Salmonella; Pa = 0.6), NA-9 (Tcruzi_amastigota; Pa = 1), NA-8 (Tcruzi_epimastigota; Pa = 1), NA-**7** (Dengue larvicida; Pa = 0.8), NAD-1 (Tripomastigote Chagas; Pa = 0.8), and NA-5 (Sars-Cov; Pa = 0.6), respectively. Whereas compounds NAD-1, NAD3-6, and NAD 8-10) and NA1-3 were biologically inactive.

Molecular docking

All 1-Piperazine indole hybrids with nicotinic amide and nicotinic acid and their derivatives are kinase inhibitors and most of the analogs are active on Trypanosomiasis (Table 5). Thus, the result of the molecular docking study of 1-Piperazine indole hybrid with nicotinic amide and nicotinic acid and

their derivatives was carried out on the crystal structure of *T. brucei* PFK complex with an allosteric inhibitor of natural product CTCB-405(JJ2) (PDB: 6QU4) by using Schrodinger Maestro-docking software as shown in Figures 2 and 3, respectively. NAD1 has the highest dock pose score (binding affinity) with PFK, as shown in Figure 3. NAD11 and NAD4 have the higher docking pose scores, respectively.

Discussion

Physicochemical, pharmacokinetic, and toxicity profile of compounds NAD 1-11 and ND 1-11

Some selected physicochemical and molecular properties, which are of high importance to the drug discovery process, were predicted using ADMETlab 2.0 https://admet-mesh.scbdd.com/.[39] Recently, we came across some interesting findings regarding the incorporation of both nicotinic amide and nicotinic acid into the indole structure. This combination has a significant impact on the physico-chemical and molecular properties of the compound. It is fascinating to see how different chemical structures can affect the properties of a substance. In our research, Table 1 illustrates four physicochemical properties that were predicted using ADMETlab 2.0.

As Table 1 shows all compounds NAD1-11 and NA1-11 and their molecular weights (MW) < 500 and most compounds of aqueous solubility (LogS) have values between −4

Table 4. Biological activity prediction of compounds (NAD 1-11 and NA 1-11) by using MolPredictX: Online tool.

Comp	Biological activity	Pa (probability active)	Pi (probability inactive)
NAD	Dengue larvicide	0	1
(Nicotinamide)	Sars-Cov	0.4	0.6
	Acetylcholinesterase	0	1
	Amastigote Ldonovani	0	1
	Tcruzi_trypomastigota	1	0
NAD1	Sars-Cov	0.2	0.8
	E_coli	0.2	0.8
	Acetylcholinesterase	0	1
	Tripomastigote Chagas	0.8	0.2
NAD2	Sars-Cov	0.2	0.8
	Salmonella	0.6	0.4
	Acetylcholinesteras	0	1
	Tcruzi_amastigota	1	0
NAD3	Dengue larvicida	0.2	0.8
	Acetylcholinesterase	0	1
	C_albicans	0	1
NAD4	Dengue larvicide	0.2	0.8
	Epimastigote Chagas	0.4	0.6
	C_albicans	0	1
	Acetylcholinesterase	0	1
NAD5	Dengue larvicida	0	1
	Acetylcholinesterase	0	1
	C_albicans	0	1
NAD6	Salmonella	0.2	0.8
	Sars-Cov	0.4	0.6
	PTR L major	0	1
	C_albicans	0	1
NAD7	Dengue larvicida	0.8	0.2
	Acetylcholinesterase	0	1
	Tcruzi_epimastigota	0	1
	C_albicans	0.4	0.6
NAD8	Dengue larvicida	0.2	0.8
	Sars-Cov	0	1
	Acetylcholinesterase	0	1
NAD9	Dengue larvicide	0.2	0.8
	Sars-Cov	0	1
	Amastigote Ldonovani	0	1
	C_albicans	0.2	0.8
NAD10	Dengue larvicida	0.2	0.8
	Acetylcholinesterase	0	1
	C_albicans	0.4	0.6
NAD11	Dengue larvicida	1	0
	Salmonella	0.4	0.6
	Sars-Cov	0	1
	Promastigote Ldonovani	1	0
NA (Nicotinic acid)	Sars-Cov	0.4	0.6
	Tcruzi_trypomastigota	1	0
	C_albicans	0	1
	Acetylcholinesterase	0	1
NA1	Dengue larvicida	0.2	0.8
	Sars-Cov	0.2	0.8
	Acetylcholinesterase	0	1

(Continued)

Table 4. (Continued)

Comp	Biological activity	Pa (probability active)	Pi (probability inactive)
NA2	Dengue larvicide	0.4	0.6
	Sars-Cov	0.4	0.6
	Lamazonensis_amastigota	0	1
	C_albicans	0	1
NA3	Acetylcholinesterase	0	1
	Dengue larvicida	0.2	0.8
	Acetylcholinesterase	0	1
	C_albicans	0	1
NA4	Sars-Cov	0.4	0.6
	Dengue larvicida	0.2	0.8
	Tcruzi_amastigota	1	0
	C_albicans	0	1
	Tcruzi_trypomastigota	1	0
NA5	Sars-Cov	0.6	0.4
	Acetylcholinesterase	0	1
	C_albicans	0	1
NA6	Sars-Cov	0.2	0.8
	Salmonella	0	1
	Acetylcholinesterase	0	1
	Tcruzi_trypomastigota	1	0
NA7	Salmonella	0.4	0.6
	Dengue larvicida	0.8	0.2
	Acetylcholinesterase	0	1
	Lamazonensis_promastigota	0	1
NA8	Sars-Cov	0.2	0.8
	Dengue larvicida	0.2	0.8
	Salmonella	0	1
	Tcruzi_epimastigota	1	0
NA9	Sars-Cov	0.2	0.8
	Dengue larvicida	0.2	0.8
	Lamazonensis_promastigota	0	1
	C_albicans	0	1
	Tcruzi_amastigota	1	0
NA10	Dengue larvicida	0.2	0.8
	C_albicans	0.6	0.4
	Acetylcholinesterase	0	1
	Tcruzi_amastigota	1	0
NA11	Dengue larvicide	1	0
	Sars-Cov	0.2	0.8
	Acetylcholinesterase	0	1
	Tcruzi_amastigota	1	0

to −2 which indicates that soluble, compounds NA1 (−1.894), NA4 (−1.99), and NA8 (−1.90) are very aqueous solubles. All compounds NAD1-11 and NA1-11 and their partition coefficient (LogP) values < 3, and n-octanol/water distribution (LogD) values < 3, the number of hydrogen bond acceptors (nHA = 5–9), number of hydrogen bond donors (nHD = 0–2), topological polar surface areas (TPSA = 41–105), number of rotatory bonds (nRot = 5–7), and number of rings (nRing = 4) and chiral centers (Stereo Centers = 0). All compounds with Lipinski's rule of five (LRO5) were accepted, and most of the compounds' quantitative estimate of drug-likeness (QED) > 0.67 indicate that they are within the normal range, but for compounds NAD11, NA3, and NA11, their QED values were 0.518, 0.665, and 0.422, respectively.

As shown in the result section, all of the compounds have passed the physicochemical properties prediction test. The scores are well within the acceptable ranges of the parameters. The molecular weight ranges from 320 to 403, which is optimal. They are moderately soluble in an aqueous medium

Table 5. Summarized biologically active analogues on disease condition and their molecular docking score.

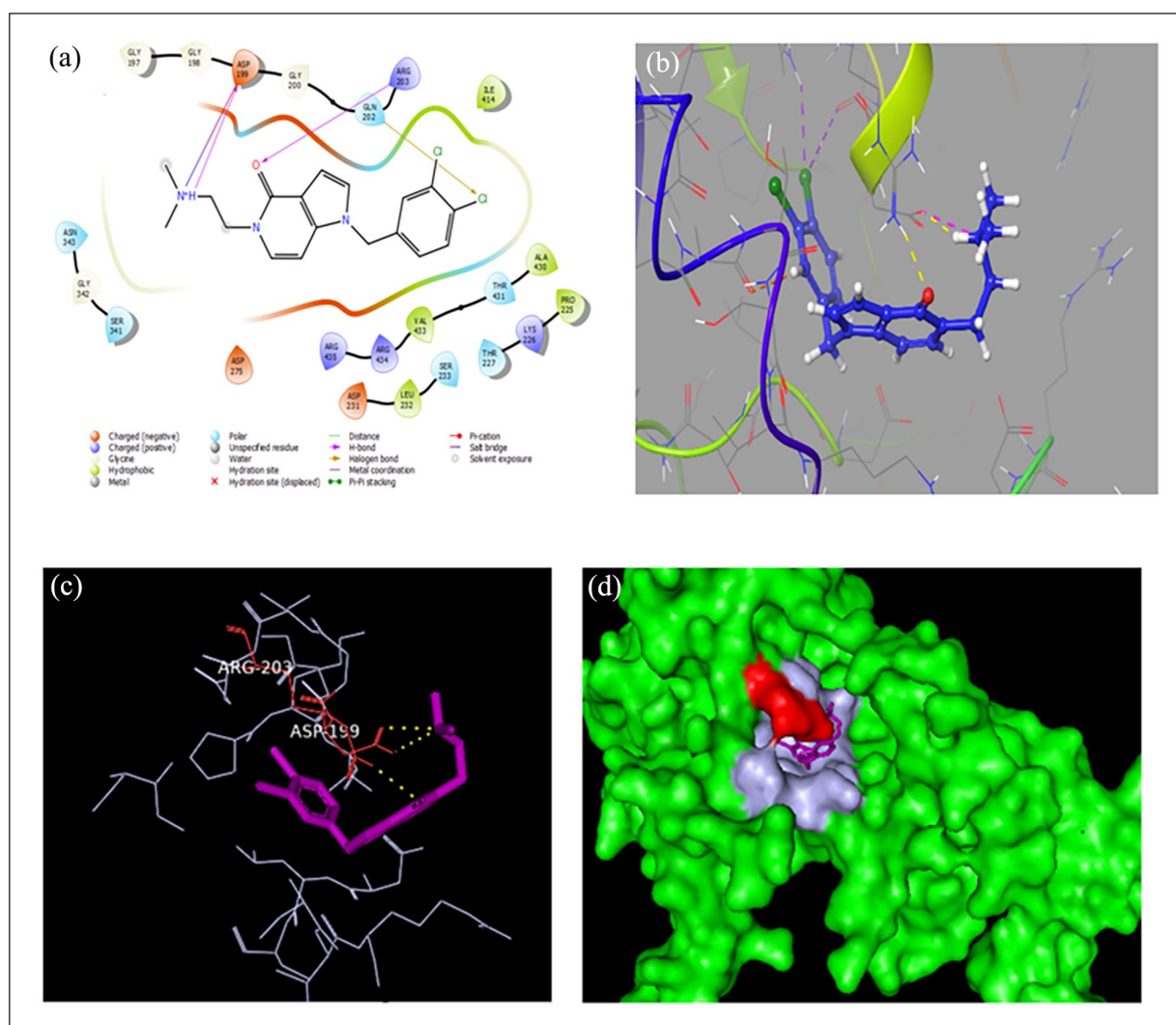| Compounds	Trypanosoma			Leishmania	Fungus	Virals		Bacterial		Docking score
	T. amastigota	T. trypomastigota	T. epimastigota	Promastigote Ldonovani	C_ albicans	Dengue larvicide	Sars-Cov	E. coli	Salmonella enterica	
NA-4	✓	✓		—	—	—	—	—	—	−5.923
NA-11	✓	—		—	—	✓	—	—	—	−6.146
NAD-11		—		✓	—	✓	—	—	—	−4.72
NA-10	✓	—		—	✓	—	—	—	—	−4.522
NAD-2	✓	—		—	—	—	—	—	✓	−5.566
NA-9	✓									−5.876
NA-8			✓							−6.406
NA-7					✓					−5.467
NAD-1			✓							−6.763
NA-5										−5.577

Figure 2. (a) 2D diagram of docked JJ2- *T. brucei* PFK chain A subunit complex. (b) 3D diagram of natural ligand JJ2 complex with the binding site of PFK. (c) Polar (Hydrogen bond) binding interaction of JJ2 with PFK amino acid residues of ARG 203 and ASP199. (d) Surface representation showing JJ2 in the binding site of PFK with lipophilicity coloring. White representing hydrophobic pockets and red representing hydrophilic pockets. JJ2 is shown in ball-stick model.
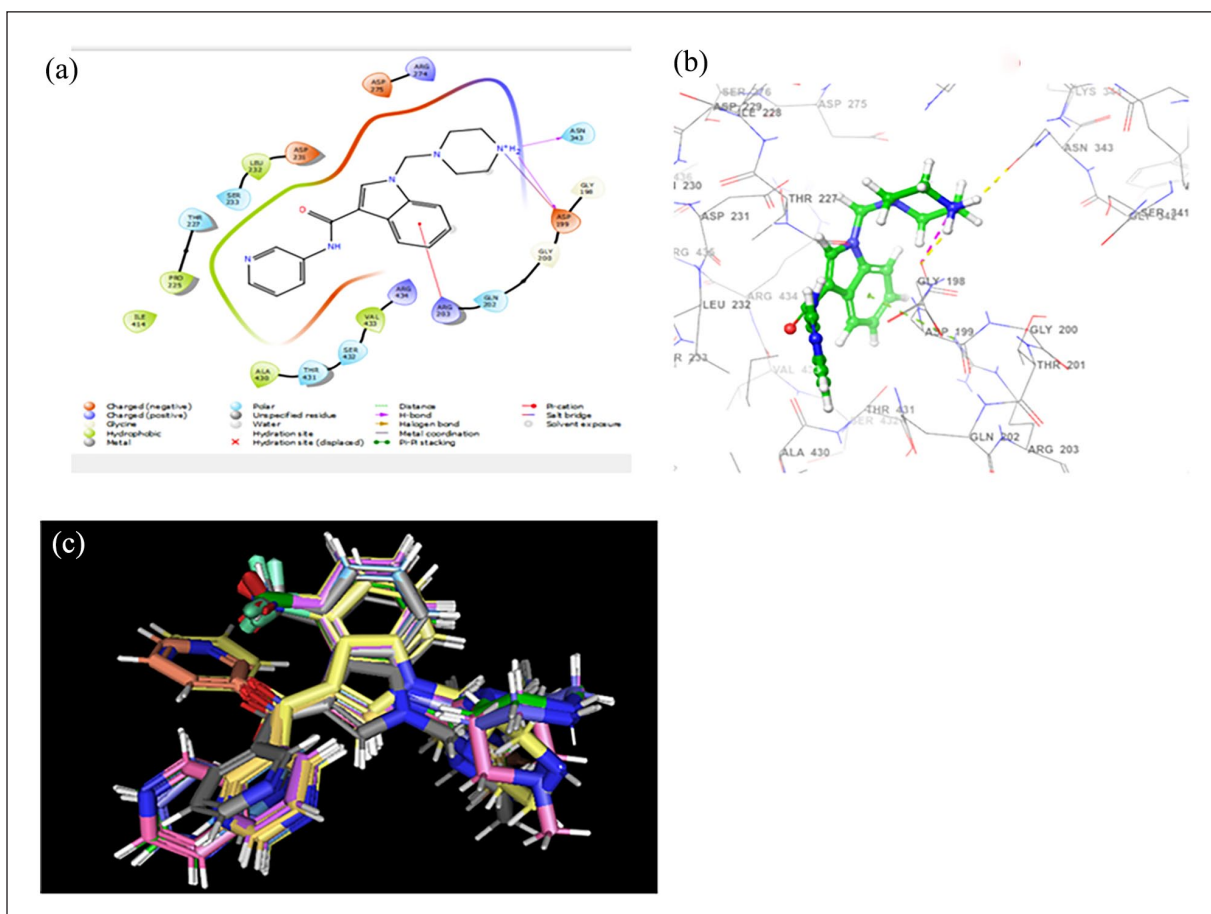
Figure 3. (a) 2D diagram of docked NAD1- *T. brucei* PFK chain A subunit complex. (b) 3D diagram of NAD1 complex with the binding site of PFK. Polar (Hydrogen bond) binding interaction of NAD1 with PFK amino acid residues of ARG 203 and ASP199. (c) The docking poses of biologically active analogues. Compounds are shown in ball-stick mode.

(LogS < −4) which indicates they have good oral absorption and easily disintegrate in the gastrointestinal tract. They also have good partition confidence (LogP 1–3) which exhibited good membrane permeability and hydrophobic binding to macromolecules. The n-octanol/water distribution coefficients are also found in the acceptable range (logD7.4 = 1–3) which indicates the compounds can enter the blood circulation and reach the site of action. All compounds obeyed the other LRO5, number of hydrogen bond donors (nHD = 0–2), number of hydrogen bond acceptors (nHA = 5–9), and topological polar surface area (TPSA = 41–105).[19]

As Lipinski's RO5 holds, these compounds follow almost all of the parameters (molecular weight (MW) < 500, the number of hydrogen bond acceptors (HBA) ⩽ 10, the number of hydrogen bond donors (HBD) ⩽ 5, and partition coefficient (LogP) value < 3) (Table 1), and they successfully passed in the evaluation of Lipinski's RO5. This is supported by similar funding reported by Al-Humaidi et al.[19]

One of the parameters used in medicinal chemistry to predict drug-likeness based on the idea of desirability is quantitative estimate of drug-likeness (QED). Compounds can be rated according to their relative merits, according to QED,

which is transparent, easy to apply, and intuitive in a variety of real-world contexts. Eight parameters associated with drug-likeness—MW, log P, nHA, nHD, PSA, nRotb, the number of aromatic rings (nAr), and the number of alerts for undesirable functional groups—are used to determine it by integrating the outputs of the desirability functions. In this case, QED was determined using average descriptor weights. The QED score is calculated by taking the geometric mean of the individual desirability functions, given by

$$QED = (exp \frac{1}{n} \sum_{i=1}^{n} \ln di)$$, where di indicates the d_{th} desirability

function and $n = 8$ is the number of drug-likeness-related properties. The mean QED is greater than 0.67 for the attractive compounds.[39,46] Based on the tool prediction, four compounds (NA3, NA4, NA11, and NAD11) failed to pass the evaluation of drug-likeness.

Pharmacokinetic and toxicity properties are essential to the drug discovery process. To estimate the pharmacokinetic and toxicological features of substances in the process of developing new drugs, we have been using ADMETlab 2.0 (Table 2). This tool has been incredibly helpful in ensuring that the compounds are safe and effective. In our study, we

meticulously evaluated 22 distinct compounds based on various pharmacokinetic and toxicity parameters. Our results indicate that several promising candidates exhibit favorable characteristics, while others may require further investigation. Overall, our findings offer valuable insights into the potential efficacy and safety of these compounds, and we hope they will inform future research in this important field. It appears that almost all of the compounds have successfully passed the pharmacokinetic evaluations. However, it seems that none of the compounds were able to pass the drug-induced liver injury (DILI) test. Out of the 22 compounds that were tested for HERG, unfortunately, five of them (NA1, NA2, NA10, NAD2, and NAD3) failed to pass. Additionally, four of the compounds (NA1, NA9, NA11, and NAD11) were unable to pass the Ames test. On a similar note, it was found that three of the compounds (NA4, NA5, and NAD4) showed carcinogenic activity.

Targets and biological activity spectrum prediction of compounds (NAD 1-11 and NA 1-11)

The prediction of bioactivity score for the most important drug targets was made using Molinspiration online tools as shown in Table 3. Most the nicotinic acid derivatives NA1-11 had the highest kinase inhibitor score (0.21–0.40), followed by nicotinic amide derivatives NAD1-11 that had a higher kinase inhibitor score (0.11–0.28). Nicotinic acid derivatives NA1-11 also had moderate enzyme inhibitors (0.07–0.25) and GPCR ligands (0.01–0.25) activity. Nicotinic amide derivatives NAD1 (0.03) and NAD6-10 (0.01–0.09) had weak GPCR ligand and enzyme inhibitors NAD1 and NAD5-10 (0.01–0.09) activity. All nicotinic acid and nicotinic amide derivatives had no activity on ion channels (−0.06 to −0.29), nuclear inhibitors (−0.18 to −0.69), and protease inhibitors (−0.17 to −0.41). Both nicotinic acid and nicotinic amide derivatives showed higher kinase inhibitor activity. Furthermore, all nicotinic acid derivatives revealed enzyme inhibitors and GPCR ligand activity. Some nicotinic amide derivatives bind at GPCR ligand (NAD1, NAD6-10) and enzyme inhibitors (NAD1, NAD5-10) activity, whereas all nicotinic acid and nicotinic amide derivatives displayed no biological activity on ion channel, protease enzymes, and nuclear receptors.

The biological activity spectra were predicted using the MolPredictX computer program as shown in Table 4. MolPredictX is an innovative and freely accessible web interface for biological activity predictions of query molecules. MolPredictX is undergoing continuous development and is freely available based on a robust analysis of structure–activity relationships in a heterogeneous training set currently including QSAR models to provide 27 qualitative predictions (active or inactive), and quantitative probabilities for bioactivity against parasitic (Trypanosoma and Leishmania), viral (Dengue, Sars-CoV and Hepatitis C), pathogenic yeast

(*Candida albicans*), bacterial (*Salmonella enterica* and *Escherichia coli*), and Alzheimer disease enzymes. The biological activity spectrum for a substance is a list of biological activity types for which the probability to be revealed (Pa) and the probability not to be revealed (Pi) are calculated.

The compound is in the biological activity spectrum since the Pa and Pi values are independent and shows that Pa > Pi for the sorts of activities compounded. The chemical is expected to show its activity in studies if Pa > 0.5. It is improbable that the compound will exhibit this activity in studies if Pa < 0.5; nevertheless, if the compound does exhibit this activity and the experiment confirms it, it may represent a novel chemical entity.[34]

The significant integration of nicotinic acid into indole structure appears to be more beneficial than nicotinic acid regarding certain biological activities, such as against Trypanosoma (Tcruzi_amastigota and Tcruzi_trypomastigota), antifungal (C_albicans), antiviral (Dengue larvicide and Sars-Cov), and Leishmania (Promastigote Ldonovani), and nicotinic acid alone does not effect on the abovementioned disease conditions as illustrated Table 4. The most biologically active compounds were the piperazine moiety of N-acetyl nicotinic acid derivative NA-4 (Tcruzi_amastigota; Pa=1 and Tcruzi_trypomastigota; Pa=1), the indole moiety of 4-nitro nicotinic acid derivatives NA-11 (Dengue larvicida; Pa=1 and Tcruzi_amastigota; Pa=1), and the piperazine moiety of N-nitro nicotinic amide derivative NAD-11 (Promastigote Ldonovani; Pa=1 and Dengue larvicida; Pa=1). Derivatives that are biologically active from highest to moderate were 4-CF$_3$ nicotinic acid derivative NA-10 (Tcruzi_amastigota; Pa=1 and C_albicans; Pa=0.6), the N-CH$_3$ nicotinic amide derivative NAD-2 (Tcruzi_amastigota; Pa=1 and Salmonella; Pa=0.6), 4-CF3 nicotinic acid derivative NA-9 (Tcruzi_amastigota; Pa=1), 4-F nicotinic acid derivative NA-8 (Tcruzi_epimastigota; Pa=1), 4-Cl nicotinic acid derivative NA-7 (Dengue larvicida; Pa=0.8), the N-H nicotinic amide derivative NAD-1 (Tripomastigote Chagas; Pa=0.8), and NA-5 (Sars-Cov; Pa=0.6), respectively, whereas nicotinic amide derivatives (NAD-1, NAD3-6, and NAD 8-10) and nicotinic acid derivatives (NA1-3) were biologically inactive.

Mechanism of action of generated compounds (NAD 1-11 and NA1-11)

According to a study by McNae et al. (2021) and based on the structural similarity of 1-Piperazine indole hybrid with nicotinic amide and nicotinic acid and its analogs and CTCB-405, inhibition of *T. brucei* phosphofructokinase (TbPFK) that blocks the glycolytic pathway result in very fast parasite kill times with no inhibition of human PFKs.[42,47] CTCB-405 is a highly specific inhibitor against the *trypanosome* PFK that blocks glycolysis in the parasite, but do not affect the human enzyme. Enzymatic and kinetic studies show that the mechanism of action is allosteric and the inhibitors do not compete with ATP in the active site. Thus, 1-Piperazine

indole hybrid, with nicotinic amide and nicotinic acid and its' analogs, a possible antitrypanosomal mechanism of action, is a TbPFK inhibitor.

Molecular docking

Molecular docking is a vital computational tool to get insight into the mechanism of action of the compounds and their binding interaction. The molecular docking score was selected by the dock poses score. The docked poses demonstrate that the drug molecules bind within the active site of the macromolecular (protein). In this study, we have used *T. brucei* PFK protein for molecular docking study. All 1-Piperazine indole hybrids with nicotinic amide and nicotinic acid and their derivatives are kinase inhibitors, and most of the analogs are active on Trypanosomiasis (Table 5). Thus, molecular docking study of 1-Piperazine indole hybrid with nicotinic amide and nicotinic acid and their derivatives were carried out on the crystal structure of *T.brucei* PFK complex with an allosteric inhibitor of natural product CTCB-405(JJ2) (PDB: 6QU4)[42]. Figure 2(a) shows a 2D diagram of docked JJ2 complex with *T.brucei* PFK chain A subunit. Figure 2(b) revealed a3D diagram of natural ligand JJ2 complex with the binding site of PFK, and Figure 2(c) shows Polar (Hydrogen bond) binding interaction of JJ2 with PFK amino acid residues of ARG 203 and ASP199. Moreover, Figure 2(d) revealed a surface representation showing JJ2 in the binding site of PFK with lipophilicity coloring (white representing hydrophobic pockets and red representing hydrophilic pockets, and JJ2 is shown in the ball-stick model).

In this funding, NAD1 has the highest dock poses score (binding affinity) with PFK, as shown in Figure 3 and Table 5 docking score. NAD11 and NAD4 have the higher docking pose scores, respectively. Figure 3(a) revealed that the 2D diagram of the docked NAD1 complex with *T. brucei* PFK chain A subunit, Figure 3(b) showed that the 3D diagram of the NAD1 complex with the binding site of PFK, and Figure 3(c) revealed the docking poses of biologically active analogs (compounds are shown in ball-stick mode). NAD1 forms two hydrogen bonds with amino acid residues Asn343 and Asp199, one salt bridge with Asp199, and pi-cation interaction with the amino acid residue of Arg203 in the binding site of 6QU4. The amino group at N-4' of the piperazine moiety of compound NAD1 forms hydrogen bonds with the side chain carbonyl oxygen of Asn343 and Asp199, respectively. Moreover, the protonated (positively charged) nitrogen of the piperazine ring forms a salt bridge with negatively charged side chain carboxylic oxygen of Asp199, suggesting its important pharmacophoric role and indole moiety forming pi-cation interaction with Arg203 amino acid.

Strengths and limitations of the study

The scientific knowledge of this study provided researchers information regarding the in silico prediction of certain pharmacokinetic, safety, biological activity, and molecular docking studies of 1-piperazine indole hybrid with nicotinic amide and nicotinic acid and their analogs, and this is one of its strongest points. This study's limitations were prolonged application setup times, virus-infected data, and unforeseen machine failures that could all result in work loss.

Conclusion

From this study, it can be concluded that all the title molecules except NAD-11, NA-1, and NA-4 were predicted to be safe regarding mutagenicity, carcinogenicity, and hepatotoxicity effects. All molecules possessed significant physicochemical, pharmacokinetic, drug-likeness, and bioactivity scores. In this study, compound NA-4 is the most active compound for Trypanosomiasis, and it has the higher molecular docking score, it serves as a lead compound, and thus we suggest further studies on its synthesis, evaluation of biological activity, and molecular models, which are necessary to improve its efficacy and safety.

Authors' contributions

Conceptualization: Melese Legesse Mitku. Data curation: Melese Legesse Mitku and Abera Dessie Dagnaw. Formal analysis: Melese Legesse Mitku and Derso Teju Geremew. Funding acquisition: Melese Legesse Mitku and Yeniewa Kerie Anagaw. Investigation: Melese Legesse Mitku, Derso Teju Geremew, and Yeniewa Kerie Anagaw. Methodology: Derso Teju Geremew, Melese Legesse Mitku, and Abera Dessie Dagnaw. Project administration: Melese Legesse Mitku, Asrat Elias Ergena and Yabibal Berie Tadesse. Resources: Melese Legesse Mitku and Minichil Chanie Worku. Software: Melese Legesse Mitku and Abera Dessie Dagnaw. Supervision: Melese Legesse Mitku, Asrat Elias Ergena, and Liknaw Workie Limenh. Validation: Melese Legesse Mitku and Abera Dessie Dagnaw. Visualization: Melese Legesse Mitku and Asrat Elias Ergena. Writing – original draft: Melese Legesse Mitku and Abera Dessie Dagnaw. Writing – review & editing: Melese Legesse Mitku and Asrat Elias Ergena.

ORCID iD

Melese Legesse Mitku (iD) https://orcid.org/0009-0001-1515-3400

Abera Dessie Dagnaw (iD) https://orcid.org/0009-0004-7805-5404

Yeniewa Kerie Anagaw (iD) https://orcid.org/0000-0001-7676-5147

Liknaw Workie Limenh (iD) https://orcid.org/0000-0002-9680-6134

References

1. Li JJ. *Heterocyclic chemistry in drug discovery*. Hoboken, NJ: John Wiley & Sons, 2013.
2. Jampilek J. Heterocycles in medicinal chemistry. *Molecules* 2019; 24(21): 3839.
3. Sravanthi T and Manju S. Indoles—a promising scaffold for drug development. *Eur J Pharmac Sci* 2016; 91: 1–10.
4. Surur AS, Huluka SA, Mitku ML, et al. Indole: the after next scaffold of antiplasmodial agents? *Drug Design Develop Ther* 2020; 14: 4855–4867.
5. Gomha SM and Riyadh SM. Synthesis under microwave irradiation of [1, 2, 4] triazolo [3, 4-b][1, 3, 4] thiadiazoles and other diazoles bearing indole moieties and their antimicrobial evaluation. *Molecules* 2011; 16(10): 8244–8256.
6. Liu F and Su M. Indole and indoline scaffolds in drug discovery. In: *Privileged scaffolds in drug discovery*. Amsterdam, The Netherlands: Elsevier, 2023, p. 147–161.
7. Alhilal S, Alhilal M, Gomha SM, et al. Synthesis and biological evaluation of new aza-acyclic nucleosides and their hydrogen complexes from indole. *Res Chem Intermed* 2022; 48(8): 3567–3587.
8. Al-Humaidi JY, Gomha SM, Riyadh SM, et al. Synthesis, biological evaluation, and molecular docking of novel azolylhydrazonothiazoles as potential anticancer agents. *ACS Omega* 2023; 8(37): 34044–34058.
9. Mahmoud E, Hayallah AM, Kovacic S, et al. Recent progress in biologically active indole hybrids: a mini review. *Pharmacol Rep* 2022; 74(4): 570–582.
10. Ibrahim MS, Farag B, Al-Humaidi JY, et al. Mechanochemical synthesis and molecular docking studies of new azines bearing indole as anticancer agents. *Molecules* 2023; 28(9): 3869.
11. Kumari A and Singh RK. Medicinal chemistry of indole derivatives: current to future therapeutic prospectives. *Bioorg Chem* 2019; 89: 103021.
12. El-Dash Y, Khalil NA, Ahmed EM, et al. Synthesis of novel nicotinic acid derivatives of potential antioxidant and anticancer activity. *Arch Pharm* 2023; 356(12): 2300250.
13. Jain N, Utreja D, Kaur K, et al. Novel derivatives of nicotinic acid as promising anticancer agents. *Mini Rev Med Chem* 2021; 21(7): 847–882.
14. Khalil NA, Ahmed EM, Mohamed KO, et al. Synthesis of new nicotinic acid derivatives and their evaluation as analgesic and anti-inflammatory agents. *Chem Pharmac Bull* 2013; 61(9): 933–940.
15. Asif M. Antimicrobial potential of nicotinic acid derivatives against various pathogenic microbes. *Eur Rev Chem Res* 2014; 1(1): 10–21.
16. Vajragupta O, Toasaksiri S, Boonyarat C, et al. Chroman amide and nicotinyl amide derivatives: inhibition of lipid peroxidation and protection against head trauma. *Free Radic Res* 2000; 32(2): 145–155.
17. Gömeç M, Nasif V, Kafa AHT, et al. Designed, synthesis, in vitro and computational analyses of anticancer nicotinamide derivatives. *Indian J Chemis* 2024; 63(2): 145–158.
18. Wen J and Shi Z. From C4 to C7: innovative strategies for site-selective functionalization of indole C–H bonds. *Acc Chem Res* 2021; 54(7): 1723–1736.
19. Al-Humaidi JY, Albedair LA, Farag B, et al. Design and synthesis of novel hybrids incorporating thiadiazole or thiazole-naphthalene: anticancer assessment and molecular docking study. *Results Chem* 2024; 7: 101475.
20. Abdelhamid AO, Gomha SM, Abdelriheem NA, et al. Synthesis of new 3-heteroarylindoles as potential anticancer agents. *Molecules* 2016; 21(7): 929.
21. Eldehna WM, Al-Rashood ST, Al-Warhi T, et al. Novel oxindole/benzofuran hybrids as potential dual CDK2/GSK-3β inhibitors targeting breast cancer: design, synthesis, biological evaluation, and in silico studies. *J Enzyme Inhib Med Chem* 2021; 36(1): 271–286.
22. Abdelhamid AO, Gomha SM and Kandeel SM. Synthesis of certain new thiazole and 1, 3, 4-thiadiazole derivatives via the utility of 3-acetylindole. *J Heterocy Chem* 2017; 54(2): 1529–1536.
23. Chen X, Zhou X-Y and Bao M. Base-catalyzed nucleophilic addition reaction of indoles with vinylene carbonate: an approach to synthesize 4-indolyl-1,3-dioxolanones. *Molecules* 2023; 28(21): 7450.
24. Candeias NR, Branco LC, Gois PM, et al. More sustainable approaches for the synthesis of N-based heterocycles. *Chem Rev* 2009; 109(6): 2703–2802.
25. Yang L, Liu Z, Li Y, et al. Electrochemically enabled C3-formylation and -acylation of indoles with aldehydes. *Org Let* 2019; 21(19): 7702–7707.
26. Kalepu J, Gandeepan P, Ackermann L, et al. C4–H indole functionalisation: precedent and prospects. *Chem Sci* 2018; 9(18): 4203–4216.
27. Hu Z, Tong X and Liu G. Rhodium (III)-catalyzed cascade cyclization/electrophilic amidation for the synthesis of 3-amidoindoles and 3-amidofurans. *Org Let* 2016; 18(9): 2058–2061.
28. Zhou W, Wang Y, Lu A, et al. Systems pharmacology in small molecular drug discovery. *Int J Mol Sci* 2016; 17(2): 246.
29. Wang J and Urban L. The impact of early ADME profiling on drug discovery and development strategy. *DDW Drug Discovery World* 2004; 5(4): 73–86.
30. Shaker B, Ahmad S, Lee J, et al. In silico methods and tools for drug discovery. *Comput Biol Med* 2021; 137: 104851.
31. Kharkar PS. Two-dimensional (2D) in silico models for absorption, distribution, metabolism, excretion and toxicity (ADME/T) in drug discovery. *Curr Top Med Chem* 2010; 10(1): 116–126.
32. Rathod SB and Vaidya VR. In silico drug discovery: a review, 2020; 9(12): 619–637.
33. Rajasekhar K, Surur AS, Mekonnen YT, et al. In silico prediction of biological activity, selected pharmacokinetic and toxicity profile of some 2, 4, 6-trisubstituted pyrimidines derived from guanabenz and guanfacine. *Inter J Innovative Pharm Res* 2015; 6: 468–477.
34. Tullius Scotti M, Herrera-Acevedo C, Barros de Menezes RP, et al. MolPredictX: online biological activity predictions by machine learning models. *Mol Inform* 2022; 41(12): 2200133.

35. Agoni C, Olotu FA, Ramharack P, et al. Druggability and drug-likeness concepts in drug design: are biomodelling and predictive tools having their say? *J Mol Model* 2020; 26: 1–11.

36. Sharma V, Sharma PC and Kumar V. A mini review on pyridoacridines: prospective lead compounds in medicinal chemistry. *J Adv Res* 2015; 6(1): 63–71.

37. Sayed AM, Khattab AR, AboulMagd AM, et al. Nature as a treasure trove of potential anti-SARS-CoV drug leads: a structural/mechanistic rationale. *RSC Adv* 2020; 10(34): 19790–19802.

38. Topliss JG. A manual method for applying the Hansch approach to drug design. *J Med Chem* 1977; 20(4): 463–469.

39. Xiong G, Wu Z, Yi J, et al. ADMETlab 2.0: an integrated online platform for accurate and comprehensive predictions of ADMET properties. *Nucl Acids Res* 2021; 49(W1): W5–W14.

40. Cheminformatics M. Calculation of molecular properties and bioactivity score, http://wwwmolinspiration com/cgi-bin/properties (2011, accessed 2023).

41. Das S, Sarmah S, Lyndem S, et al. An investigation into the identification of potential inhibitors of SARS-CoV-2 main protease using molecular docking study. *J Biomol Struct Dynam* 2021; 39(9): 3347–3357.

42. McNae IW, Kinkead J, Malik D, et al. Fast acting allosteric phosphofructokinase inhibitors block trypanosome glycolysis and cure acute African trypanosomiasis in mice. *Nat Commun* 2021; 12(1): 1052.

43. Sahayarayan JJ, Rajan KS, Vidhyavathi R, et al. In-silico protein-ligand docking studies against the estrogen protein of breast cancer using pharmacophore based virtual screening approaches. *Saudi J Biol Sci* 2021; 28(1): 400–407.

44. Nomura R, Nakano K, Nemoto H, et al. Isolation and characterization of streptococcus mutans in heart valve and dental plaque specimens from a patient with infective endocarditis. *J Med Microbiol* 2006; 55(8): 1135–1140.

45. Arévalo MP, Carrillo-Muñoz A-J, Salgado J, et al. Antifungal activity of the echinocandin anidulafungin (VER002, LY-303366) against yeast pathogens: a comparative study with M27-A microdilution method. *J Antimicrob Chemother* 2003; 51(1): 163–166.

46. Bickerton GR, Paolini GV, Besnard J, et al. Quantifying the chemical beauty of drugs. *Nat Chem* 2012; 4(2): 90–98.

47. Musanabaganwa C and Byiringiro F. Anti-trypanosomal activity of potential inhibitors of trypanosoma brucei glycolytic pathway enzymes selected by docking studies. *Rwanda Med J* 2014; 71: 13–17.